Nano World Journal

https://doi.org/10.17756/nwj.2023-s3-121

Research Article

Open Access

# Enhancing Radiator Efficiency with Hybrid Nanofluids: A Comparative Study of SiC-Graphene and CNT-Graphene Compositions

**A.H. Alkkhayat[1], Indira Gomathinayagam[2*], Padmavathy[3], Ahmed H.R. Abbas[4], I. B. Sapaev4 and Senthil Kumar Rengasamy[5]**

[1]*College of Technical Engineering, The Islamic University, Najaf, Iraq*
[2]*Department of Electrical and Electronics Engineering, Prince Shri Venkateshwara Padmavathy Engineering College, Chennai, Tamil Nadu, India*
[3]*Department of Electronics and Communication Engineering, New Prince Shri Bhavani College of Engineering, Chennai, Tamil Nadu, India*
[4]*Head of the department Physics and Chemistry, Tashkent Institute of Irrigation and Agricultural Mechanization Engineers, National Research University, Tashkent, Uzbekistan, Western Caspian University, Scientific researcher, Baku, Azerbaijan*
[5]*Department of Mathematics, AAA College of Engineering and Technology, Sivakasi, Tamil Nadu, India*

***Correspondence to:**
Indira Gomathinayagam
Department of Electrical and Electronics Engineering,
Prince Shri Venkateshwara Padmavathy Engineering College,
Chennai, Tamil Nadu, India.
**E-mail:** g.indira_eee@psvpec.in

**Received:** July 28, 2023
**Accepted:** October 27, 2023
**Published:** October 31, 2023

**Citation:** Alkkhayat AH, Gomathinayagam I, Padmavathy, Abbas AHR, Sapaev IB, et al. 2023. Enhancing Radiator Efficiency with Hybrid Nanofluids: A Comparative Study of SiC-Graphene and CNT-Graphene Compositions. *NanoWorld J* 9(S3): S666-S676.

**Copyright:** © 2023 Alkkhayat et al. This is an Open Access article distributed under the terms of the Creative Commons Attribution 4.0 International License (CCBY) (http://creativecommons.org/licenses/by/4.0/) which permits commercial use, including reproduction, adaptation, and distribution of the article provided the original author and source are credited.

Published by United Scientific Group

## Abstract

The thermal performance analysis of a radiator was tested with three different types of nanoparticles: cylindrical (CNT)-platelet (graphene), spherical (SiC), and a hybrid fluid based on spherical (SiC) and cylindrical (CNT) composition. The experimental conditions included a coolant flowrate (CFR) of 7.1 L/min, an air velocity of 12.8 m/s, and a volume fraction of 1.6% hybrid nanofluid (HNF). An improvement in the exergy-energy performance of radiators was observed when coolants made of HNFs were used. Researchers found that when tested with different CFR and air velocities, spherical (SiC)-platelet (graphene) HNFs performed better than cylindrical (CNT)-platelet (graphene) hybrids. The irreversibility, second law efficiency, and energy change are all affected by the shape of the particles, and this effect becomes more pronounced as the air velocity and volume percentage of the HNF increase. The spherical (SiC)-platelet (graphene) HNF outperforms its cylindrical (CNT)-platelet (graphene) counterpart in terms of performance index (PI), exergy changes in coolant efficiency (3.9%), and second law efficiency (1.44%). According to the findings, the shape of the nanoparticles significantly affects how well a car radiator works. The spherical (SiC)-platelet (graphene) HNF outperforms other shapes when it comes to thermal performance, making it an excellent radiator coolant.

## Keywords

Thermal systems, Platelet, Hybrid nanofluid, Heat exchangers, Nanoscale heat transfer

## Introduction

A radiator is used by the vehicle's engine to dissipate any surplus heat. Avoiding component failure due to overheating is the primary goal of the research, which is why radiator performance is also closely monitored [1]. The term "Nanofluid" describes a mixture of metals or metal oxides with a size smaller than 100 nm that is added to a regular fluid [2]. Even at low immersion concentrations, the net thermal conductivity is improved due to the large surface area that emerges from nanoparticles' diminutive size [3, 4]. Still, the radiator is a heat exchanger that releases the energy stored in the engine's coolant onto the surrounding air. For radiator performance, there are some known traditional research, wavy fin structures allow for better energy transfer than flat fin structures because of their increased surface area and the fact that they can reconstruct a thin boundary layer all the way through the passage; researchers have also looked at the performance of louvred H-type wavy fin structures [5, 6].

The author found that using a combination of nanofluid with a wavy structure and regular fluid increases heat transmission by around 100% [7, 8]. Thermophysical characteristics of the chosen nanoparticles and the working base fluid determine the thermohydraulic performance [9]. When it comes to heat exchanger performance, factors such as coolant type, nanoparticle shape, size, and concentration are crucial [10]. According to research by authors [11], which examined how various forms affected heat exchanger performance, shape is a key factor in determining performance. In addition, researchers conducted research on a wavy fin and tube radiator using water as a base fluid and various nanoparticle shapes. The results showed that spherical and cylindrical nanoparticles were the best options for the coolant medium.

In addition, authors [12] showed that, while studying the form effect on shell and tube heat exchangers, the most thermo-economic improvement was observed in nanofluids with a brick shape, followed by those with a blade, cylindrical, or platelet shape. Nevertheless, authors [13] showed that the shape is a major factor affecting the heat exchanger's performance. In a similar way, authors [14] examined the performance of five distinct nanoparticle shapes on heat exchanger with respect to heat transmission and rate of entropy formation. They found that the cylindrical shape performed the best. There is an abundance of literature on energy performance, but a dearth of literature on exergy analysis. Researchers [15] examined the nanofluid flow of silica water composition in conventional, mini channel, and micro-channel systems and found that addition of nanoparticles to water increases entropy generation in those channels.

In contrast, authors [16] observed that, while studying the energy and exergy of fluid flow in the heat exchanger with walls, viscous irreversibility is more prominent at the duct's core, whereas thermal entropy generation was more responsible for irreversibility near the walls. Nevertheless, authors [17] demonstrated an increase in heat transfer after investigating the energy analysis with nanofluid. While references detailed heat transfer analyses across heat exchangers, only a small number of research found that nanoparticle shape and concentration affected thermal performance.

The major emphasis of this research is the impact of HNF compositions on the performance of wavy fin and tube radiators. These compositions principally consist of cylindrical (CNT)-platelet (graphene), spherical (SiC)-platelet (graphene), and spherical (SiC)-CNT nanoparticles. The effect of various HNFs based on particle shape on the efficiency of car radiators is the focus of this research. Radiators of various shapes, including spherical, cylindrical, and hybrid platelet forms, have also been subjected to exergy and energy assessments. Research and comparisons have been conducted on a number of performance metrics, including heat transfer rate, efficacy, and PI. CFR, volume fraction of HNF, and ambient air velocity are the characteristics that have been studied in the exergy study, which includes irreversibility, second law efficiency, entropy generation, and exergy change. In addition, the morphological examinations of the various HNFs based on nanoparticles are encompassed in the present analysis.

# Methodology

## Mathematical modeling

Table 1 lists geometrical configurations assessed using laboratory instruments. Radiators that use water as their main fluid and incorporate various shaped nanoparticles, such as spherical (SiC)-platelet (graphene), spherical (SiC)-CNT, and CNT-platelet (graphene), have had their performance evaluated. Under the following assumptions, the exergy and energy assessments were conducted on a radiator operating in a steady-state, steady-flow condition:

- There is no way for the radiator to generate or dissipate heat.
- Air is used to absorb the heat that is generated by the coolant.
- The property is determined at the mean temperature and is independent of temperature variations.
- Ignoring wall resistance.

### Airside analysis

According to authors [18], the wavy fin's Colburn factor (CF) equals

$$\mathrm{CF} = \frac{1.201}{\ln\left(\mathrm{Re}_a^{2.921}\right)} \tag{1}$$

Reynold's number and mass velocity of air

$$\mathrm{MV}_a = \frac{m_a}{A_{fr}} \text{ and } \mathrm{Re}_a = MV_a * D_a/\mu_a \tag{2}$$

Coefficient of heat transfer for airside

$$h_a = \frac{\mathrm{CF} * \mathrm{MV}_a * cp_a}{\mathrm{Pr}_a^{2/3}} \tag{3}$$

Radiator efficiency with wavy fins

$$\eta_f = \frac{\tanh\left(mr\theta\right)}{mr\theta} \tag{4}$$

Where

$$\beta = \left(\frac{\mathrm{R}_{eq}}{r} - 1\right) * \left(1 + 0.35\left(\ln\frac{\mathrm{R}_{eq}}{r}\right)\right) \tag{5}$$

$$\frac{\mathrm{R}_{eq}}{r} = 1.27 * \left(\frac{Y_l}{Y_m} - 0.3\right)^{0.5} \tag{6}$$

$$Y_m = P_l/2 \text{ and } Y_l = \sqrt{\left(\frac{P_t}{2}\right)^2 + \left(\frac{P_l}{2}\right)^2} \tag{7}$$

According to [19], rate of airside heat capacity is:

$$C_a = \rho_a * V_a * A_{fr} * cp_a \tag{8}$$

### Coolant-side performance

The specific heat capacity and density of a fluid were dependent on nanoparticle concentration in volume. The individual attributes of the particles are reported in table 2,

**Table 1:** Design dimension of a wavy fin radiator.

| Description | Coolant side | Air side |
|---|---|---|
| Fin thickness | - | 0.15 |
| Fin pitch | - | 3.7 |
| Outside diameter | 10.12 | - |
| Longitudinal pitch | - | 19.6 |
| Tube thickness | 0.21 | - |
| Core height (H) | - | 410 |
| Transverse pitch | - | 24.8 |
| Core depth (D) | - | 84 |
| Tube Length (L) | 460 | - |
| Fin area | - | 0.84 |
| Free flow area/frontal area | 0.129 | 0.78 |
| Tube arrangement | Staggered | - |

**Table 2:** Thermophysical characteristics of nanoparticles and water [25].

| Properties | Unit | CNT | Water | SiC | Graphene |
|---|---|---|---|---|---|
| Shape | | Cylindrical | - | Spherical | Platelet |
| ρ | kg/m$^3$ | 2100 | 997.1 | 3970 | 2200 |
| β | 1/K | 0.00002 | 0.00021 | 5.80E-06 | -0.000008 |
| k | W/m.K | 3007.4 | 0.613 | 40 | 5000 |
| $c_p$ | J/kg.K | 410 | 4179 | 765 | 790 |

though, therefore effective specific heat and density using mixture model [20] are provided as:

$$\rho_{hnf} = \rho_1\alpha_1 + \rho_2\alpha_2 + \left(1-\alpha_1-\alpha_2\right)\rho_{bf} \quad (9)$$

$$\left(\rho_{hnf}c_p\right)_{hinf} = \rho_1 c_{p,1}\alpha_1 + \rho_2 c_{p,2}\alpha_2 + \left(1-\alpha_1-\alpha_2\right)\left(\rho_{bf}c_{p,bf}\right) \quad (10)$$

In addition to the volume concentration of particles, their form (cylindrical, platelet, or blade) affects fluid flow properties such as dynamic viscosity and thermal conductivity. This study considers nanoparticles in two forms: volume concentration and shape. Nanofluids with identical nanoparticles of any shape can have their thermal conductivity determined using Maxwell-Garnett model [21].

$$\frac{K_{nf1}}{K_{bf}} = \frac{k_1 + (n-1)k_{bf} + (n-1)\alpha\left(k_1 - k_{bf}\right)}{k_1 + (n-1)k_{bf} - \left(k_1 - k_{bf}\right)} \quad (11)$$

Where $n$ = 3/Ψ, form factor (n) and sphericity (Ψ), which is calculated as the proportion at equal volumes of the real particle surface area to the surface area of a sphere. Ψ = 0.55, $n$ = 6.0 for nanoparticles with a platelet shape; Ψ = 0.7.244, $n$ = 4 for nanoparticles with a cylindrical shape [22].

Accordingly, authors provide thermal conductivity for nanoparticles with a cylindrical, platelet, or spherical shape.

$$\frac{K_{nf1}}{K_{bf}} = \frac{k_1 + 2k_{bf} + 2\phi\left(k_1 - k_{bf}\right)}{k_1 + 2k_{bf} - \left(k_1 - k_{bf}\right)} \quad (12)$$

(nanoparticle-of spherical shape)

$$\frac{K_{nf2}}{K_{bf}} = \frac{k_2 + 3.9k_{bf} + 3.9\alpha\left(k_2 - k_{bf}\right)}{2k_1 + 3.9k_{bf} - \left(k_2 - k_{bf}\right)} \quad (13)$$

(nanoparticle-2 of cylindrical shape)

$$\frac{K_{nf2}}{K_{bf}} = \frac{k_2 + 4.7k_{bf} + 4.7\alpha\left(k_2 - k_{bf}\right)}{2k_1 + 4.7k_{bf} - \left(k_2 - k_{bf}\right)} \quad (14)$$

The viscosities of HNFs with nanoparticles of varying shapes are also provided by [23]:

$$\mu_{nf1} = \mu_{bf}\left(1 + 2.5\phi + \phi^2\right) \quad (15)$$

$$\mu_{nf2} = \mu_{bf}\left(1 + 13.5\alpha + 904.4\alpha^2\right) \quad (16)$$

(nanoparticle-2 of cylindrical shape)

$$\mu_{nf2} = \mu_{bf}\left(1 + 37.1\alpha + 612.6\alpha^2\right) \quad (17)$$

(nanoparticle-2 of platelet shape)

Various nanoparticle forms were used to assess the nanofluid's viscosity and thermal conductivity. The HNFs effective dynamic viscosity with a concentration of 1 for nanoparticle-1 and 2 for nanoparticle-2, as well as a total concentration, may be determined by using the interpolation approach.

$$\mu_{hnf} = \left(\mu_{nf1}\alpha_1 + \mu_{nf2}\alpha_2\right)/\alpha \quad (18)$$

Similarly, the HNFs thermal conductivity was found for nanoparticles with different shapes by utilizing the interpolation method.

$$k_{hnf} = \left(k_{nf1}\alpha_1 + k_{nf2}\alpha_2\right)/\alpha \quad (19)$$

## Performance analysis

The coolant-side heat capacity was given by:

$$C_f = \rho_f V_f cp_f \quad (20)$$

The pressure drop of coolant is defined as

$$\Delta p_f = \left[\mathrm{MV}_f^2 \text{ x } f_f \text{ x } H_c\right]/2 \text{ x } \rho_f \text{ x } \left(D_{h,f}/4\right) \quad (21)$$

When the friction factor has been determined using appropriate correlations [24]; The entire heat transfer coefficient is now stated as.

$$\frac{1}{\mathrm{UA}} = \frac{1}{\eta_o h_a A_a} + \frac{1}{h_f A_f} \quad (22)$$

Those have been determined to have an effective surface temperature by

$$\eta_o = 1 - \frac{A_{fin}}{A_a}\left(1 - \eta_{fin}\right) \quad (23)$$

This is the expression for the effectiveness of crossflow unmixed fluid:

$$\varepsilon = 1 - \exp\left[\frac{\mathrm{NTU}^{0.22}}{C^*}\exp\left(-C^*\,\mathrm{NTU}^{0.78} - 1\right)\right] \quad (24)$$

The overall rate of heat transport is calculated by:

$$Q = \varepsilon C_{\min}\left(T_{f,in} - T_{a,in}\right) \quad (25)$$

The power required to pump coolant is:

$$P_P = V_f * \Delta P_f \quad (26)$$

The airside pressure drop is:

$$\Delta p_a = \frac{MV_a^2}{2\rho_{a,i}}\left[\left(1+\sigma^2\right)\left(\frac{\rho_{a,i}}{\rho_{a,e}}-1\right)+f_a\frac{2F_d}{D_{h,a}}\left(\frac{\rho_{a,i}}{\rho_{a,e}}+1\right)\right] \quad (27)$$

The power of the fan has since been determined by:

$$P_f = A_{fr} * u * \Delta P_a / \eta_f \quad (28)$$

A definition of the PI is now possible with:

$$\mathrm{PI} = \frac{Q}{P_P + P_F} \quad (29)$$

The exergy and entropy of fin radiator was assessed according to performance of heat exchanger criteria requirements. The radiator entropy was understood by comparing the compressibility of the pneumatic medium with that of the incompressible fluid medium that flows across the radiator, the coolant. Hence, the creation of radiator entropy can be calculated as:

$$\dot{S}_{gen} = \dot{m}_a\left[c_{pa}\ln\frac{T_{a,e}}{T_{a,i}} - R_a\ln\frac{p_{a,e}}{o_{a,i}}\right] + \dot{m}_f\left[c_{pf}\ln\frac{T_{f,e}}{T_{f,i}} - \frac{p_{a,e}-p_{a,i}}{\rho_f T_{f,mean}}\right] \quad (30)$$

If one follows the procedures outlined by authors, the radiator's entropy generation number was determined by:

$$N_s = S_{gen}/C_{\max} \quad (31)$$

The exergy loss caused by the coolant is:

$$\Delta Ex_f = Q - T_0\left[\dot{m}_f c_{pf}\ln\left(T_{f,i}/T_{f,e}\right) - \dot{m}_f\Delta p_f/\left(\rho_f T_{f,mean}\right)\right] \quad (32)$$

While the rate of exergy acquisition by air is determined:

$$\Delta Ex_a = Q - T_0\left[\dot{m}_a c_{pa}\ln\left(T_{a,e}/T_{a,i}\right) + \dot{m}_a R\ln\left(p_{a,i}/p_{a,e}\right)\right] \quad (33)$$

If the dimensionless exergy loss is given by $I^* = I/Q_{\max}$, then:

$$I^* = \frac{N_s}{C^*}\frac{T_0}{T_{f,i}-T_{a,i}} \quad (34)$$

The efficiency provided by the second law is:

$$\eta_2 = \frac{\Delta EX_a}{\Delta Ex_f} \quad (35)$$

Finally, the efficiency index is assessed using the formula:

$$\mathrm{EI} = \frac{\mathrm{CF}}{f} \quad (36)$$

## Methodology and result validation

The mean fluid temperature and thermophysical characteristics of the air and coolant were estimated by analyzing the aforementioned theoretical coupled equations with Engineering Equation Solver. Iterations were performed for fluid properties that are dependent on average temperature since outlet temperatures were desired estimate of the simulated outcomes. Figure 1 shows the simulation method of path process used to determine the different results. Using the mixture model technique, we predicted the inlet temperatures (Tci = 85 °C and Tai = 35 °C) and nanoparticle characteristics at 1% volume fraction of nanofluid, taking into account the data from table 2. After the airside and coolant-side convective coefficients were known, the total heat transfer was calculated using the ε-number of transfer units (NTU) approach in the Engineering Equation Solver. Then, the performance parameters that resulted were examined.

Experimental results of spherical shape under steady-state conditions were used to validate the numerical code for a HNF based on spherical-platelet form nanoparticles. In an experimental setting involving a nanofluid based on spherical nanoparticles, the outcomes were contrasted with the accessible set of variables. Figure 2 illustrates that the coolant outlet temperature and heat transfer follow a similar trend, with a maximum variance of 6% and 5% between the experimental and predicted results.

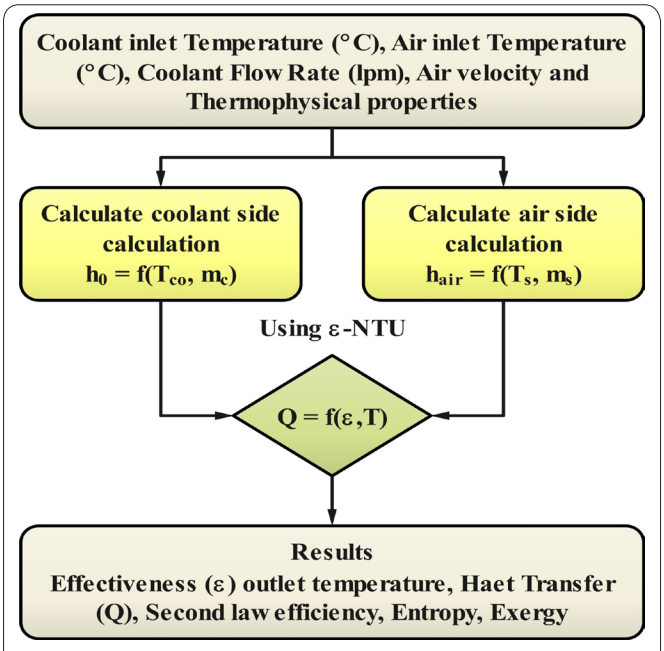



**Figure 1:** The process flow diagram for numerical simulation.

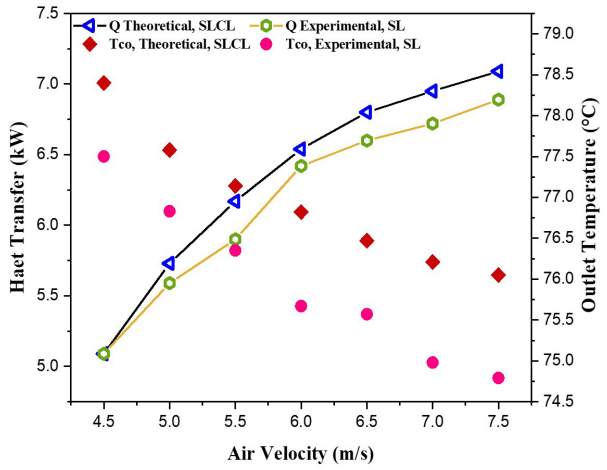



**Figure 2:** Comparing the outcomes of the simulations to those of theoretical and experimental studies.

# Results and Discussion

## Impact of parameter on PI and effectiveness

A wavy fin radiator was designed to use a water based HNF as a coolant. This fluid might have a spherical (SiC)-platelet (graphene), spherical (SiC)-cylindrical (CNT), or cylindrical (CNT)-platelet (graphene) structure. Figure 3, figure 4, and figure 5 show the effects of changing the PI and effectiveness on the flowrate of coolant, the velocity of air, and the volume percentage of the HNF. For a wavy fin radiator with 0.02 m hydraulic diameter, the outcomes showed a consistent rise in efficiency with the volume fraction of air velocity and HNF.

When tested at a speed of 12.89 m/s, the HNF based on cylindrical and platelet-shaped particles was 9.4% more effective than the spherical-platelet-based HNF and 4.2% higher than the spherical-cylindrical HNF. In addition, the spherical-platelet shape particle demonstrated its greatest efficacy as the volume percentage increased, owing to its larger heat transfer coefficient. Despite a moderate decrease in effectiveness with increasing CFR, the hybrid composition nanofluid containing cylindrical-platelet shape particles outperforms both the spherical-platelet and spherical-cylindrical shape particle-based nanofluids by 6.6% and 3.2%, at 7.1 L/min flow rate. One possible explanation is that with increasing flowrates, the heat capacity increases. However, as the HNFs volume fraction and CFR rise, the PI also rises. Under 7.1 L/min, the outcomes illustrated that the PI of spherical-platelet shape-based HNF is 3.5% greater than that of the cylindrical-platelet shape and 1.6% greater than that of the spherical-cylindrical HNF. The reduced pumping force can be to blame for this if the viscosity is low. The PI rises up to 4 m/s of air velocity before the dominance of fan power causes an occasional decrease in PI due to the fact that increasing the air velocity increases the fan power with no change in heat transfer. Moreover, at an air velocity of 3.4 m/s, the PI of the cylindrical-platelet HNF is 19.2% greater than that of the spherical-platelet hybrid and 7.9% greater than that of the spherical-cylindrical hybrid. Lower air velocities have been found to produce the best increases in PI.

## Effect of parameter on entropy change and generation in air

Figure 6, figure 7, and figure 8 display the air entropy generation in proportion to the air velocity, fraction of HNF, volume, and CFR, as well as the effect of varying these factors. The air entropy shift becomes increasingly noticeable for a wavy fin radiator with a hydraulic diameter of 0.01 m as the CFR, air velocity, and volume fraction of HNF rise. At 7.1 L/min of CFR, the spherical-platelet HNF showed a 5.5% larger entropy change than the cylindrical-platelet HNF, while the spherical-cylindrical hybrid came out in the middle. An increase in viscous entropy creation leads to an increase in the entropy change, which in turn causes such variations with the parameters. On the other hand, when it comes to thermal system design, a low entropy requirement is ideal. The spherical-platelet HNF may have a greater heat transfer coefficient than other shapes of HNFs, but it has a higher entropy change in air for the same volume fraction of nanofluid. The entropy change of air is 4.3% larger in the blade-platelet shape-based HNF compared to the cylindrical-platelet HNF, and this is because the viscous entropy increases with increasing air velocity. On the other hand, a spherical-cylindrical HNF with 12.8 m/s air velocity produced an intermediate outcome.

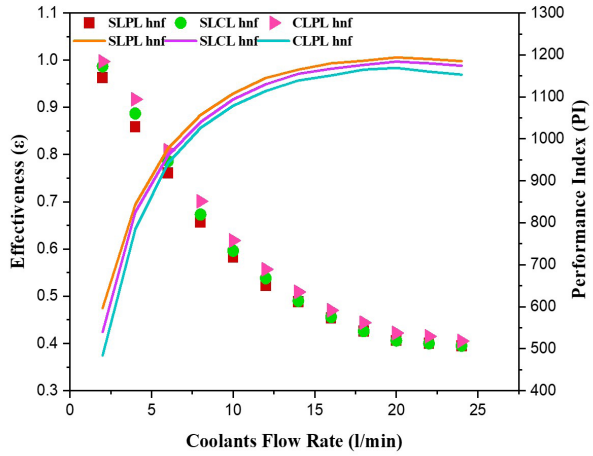



**Figure 3:** Effectiveness and PI with CFR.

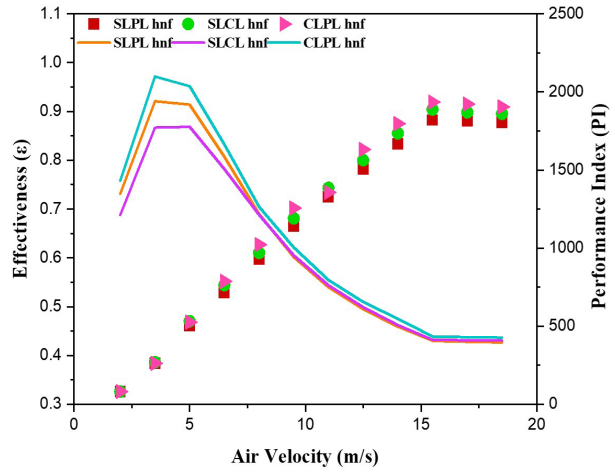



**Figure 4:** PI and effectiveness with air velocity.

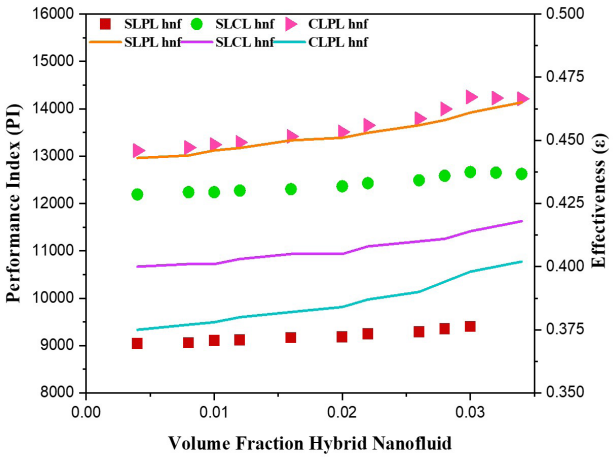



**Figure 5:** PI and effectiveness with volume fraction of HNF.

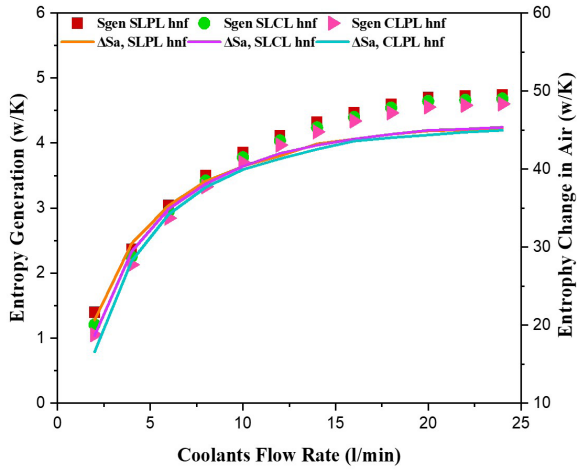



**Figure 6:** Entropy variation in air and entropy production with CFR.

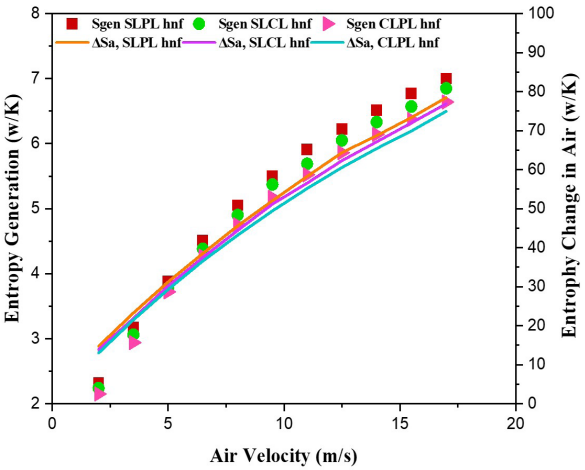



**Figure 7:** Entropy variation in air and entropy production with the air velocity.

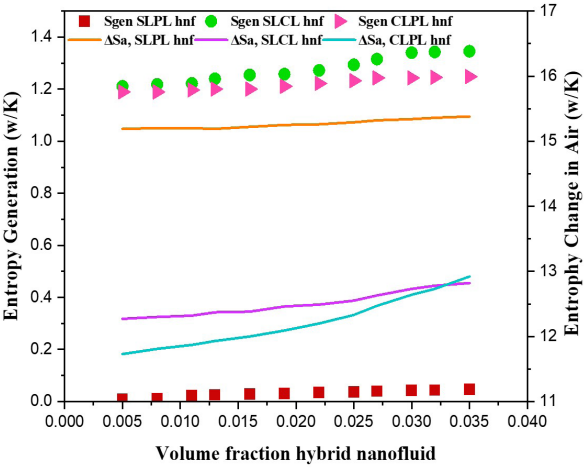



**Figure 8:** Entropy variation in air and entropy production with volume fraction of HNF.

For a wavy fin radiator, the best thermal coolant is the one that minimizes entropy formation. Findings showed that as the CFR, volume fraction and air velocity, of the HNF increase, the entropy generation also increases. Also, for the same reason as with entropy change, the spherical-platelet HNF generates 3.6% more entropy than the cylindrical-platelet HNF at CFR of 7.1 L/min. By minimizing entropy, a more energy-efficient system is constructed. In addition, the entropy creation is affected by volume fraction of nanoparticles; lower volume proportion of HNF results in less entropy generation than a higher volume fraction. Additionally, at 12.89 m/s air velocity, it was found that the spherical-platelet HNF increased entropy generation by 6.2% and the spherical-cylindrical HNF by 2.4% when compared to the cylindrical-platelet HNF. One alternative to conventional coolants for wavy fin radiators is a HNF based on a cylindrical-platelet shape, which has the advantage of generating the fewest possible entropy.

## Effect of the parameter on exergy change in air and exergy change in coolant

Figure 9, figure 10, and figure 11 show the required second law analysis for minimum entropy and mean entropy, as well as the effects of air velocity, CFR, exergy change in air and coolant and volume fraction of HNF, on each other. At an air velocity of 4 m/s, the exergy change in the air and the exergy change in the coolant both rise with the CFR and the volume fraction of the HNF in a wavy fin radiator. The exergy increase with CFR is due to the rise in viscous entropy, which is caused by an increase in CFR; however, the viscosity is still predominated by the addition of particles to the coolant. At 7.1 L/min, the blade-platelet shaped nanoparticles exhibit a 3.6% greater exergy change in the coolant compared to the cylindrical-platelet HNF. On the other hand, at the same flowrate, the spherical platelet nanoparticles exhibit a 2.9% higher exergy change in air compared to cylindrical-platelet HNF.

Case spherical-platelets outperform other shapes in terms of exergy change in coolant and air, even when considering volume percentage of HNF. Another factor that contributes to an increase in exergy is the speed of the air. In addition, at 12.8 m/s air velocity, the spherical-platelet nanoparticle exhibits a 4.2% greater exergy change in coolant compared to the cylindrical-platelet HNF. At the same air flowrate, the blade-platelet shape outperforms the cylindrical-platelet hybrid by 5.08%. Meanwhile, the spherical-cylinder HNF changed air and coolant exergy to a medium degree when compared to others.

## Effect of parameters on exergy loss and entropy generation number

In order to compensate for the extra labor or power input, two crucial parameters are entropy generation number and exergy loss determination. Figure 12 to figure 15 show the relationship between volume fraction of HNF, air velocity, CFR, and the variation in exergy loss and number of entropy generation. Together, irreversibility and heat transfer form a dimensionless exergy loss dependency. There is a strong correlation between the ratio of irreversibility and heat transfer, and this correlation grows as the volume percentage of HNF and air velocity increases. However, when CFR increases, irreversibility and heat transfer both increase; however, as heat transfer becomes more dominant, their ratio drops, leading to a reduction in exergy loss.

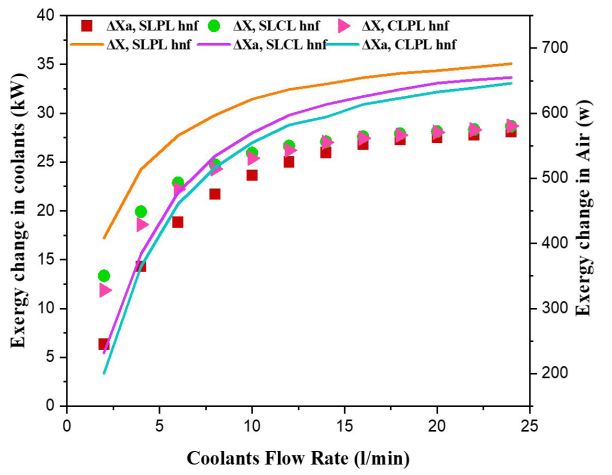



**Figure 9:** Air energy change and coolant energy change using CFR.

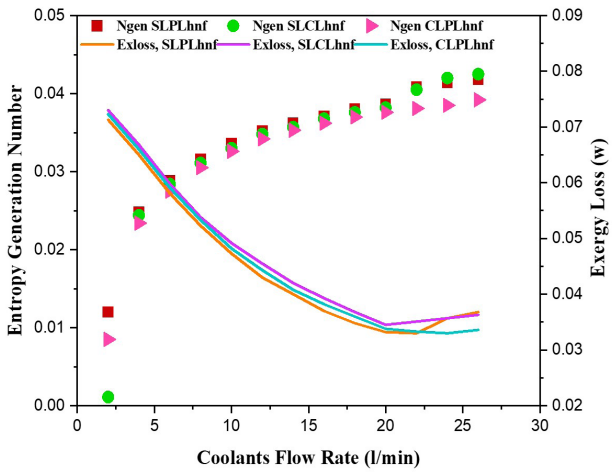



**Figure 12:** Entropy generation number and exergy loss with CFR.

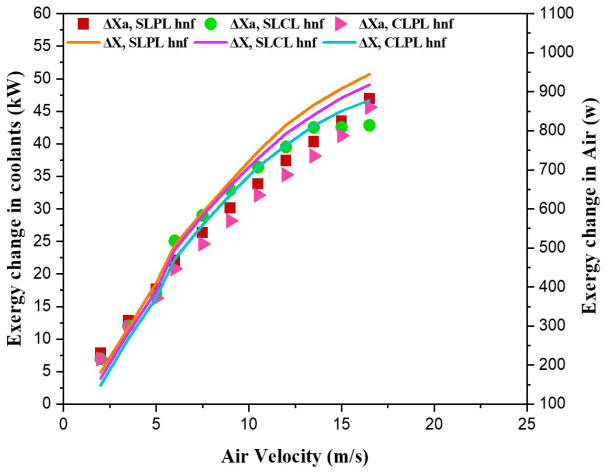



**Figure 10:** Variation in exergy of air and coolant with air velocity.

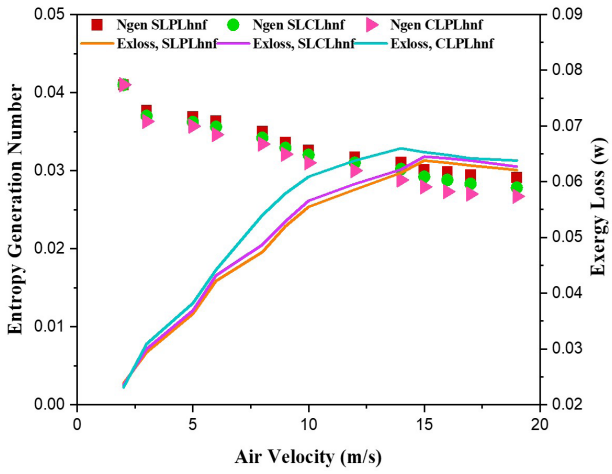



**Figure 13:** Entropy generation number and exergy loss with air velocity.

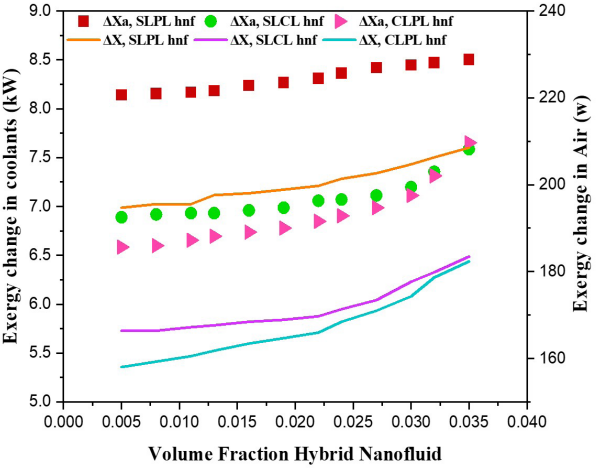



**Figure 11:** Air and coolant energy changes in relation to HNF volume fraction.

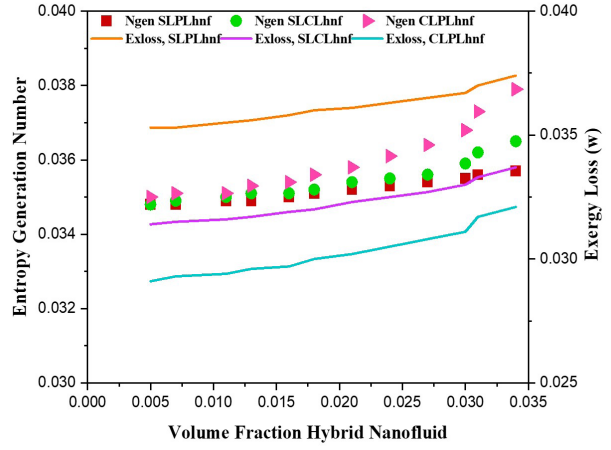



**Figure 14:** Entropy generation number and exergy loss with volume fraction of HNF.

While the spherical-cylindrical HNF does have some exergy loss, the results showed that at 7.1 L/min CFR and an air velocity of 12.8 m/s, respectively, the exergy loss was 4.1% lower in the spherical-platelet-based and 3.9% lower in the cylindrical-platelet-based HNFs. At 1.6% volume fraction in fin radiator, the exergy loss was 17.34% lower for the

spherical-cylindrical HNF compared to the spherical-platelet HNF. This difference was observed when the volume fraction was changed. As the dominant effect of irreversibility reduces available production, exergy loss increases with increasing air velocity.

A HNF based on spherical platelet composition shows a 2.7% reduced exergy loss at a speed of 15 m/s compared to a cylindrical platelet composition. As the net entropy generation rises, the entropy generation number grows with the CFR and volume fraction of the HNF. Nevertheless, the entropy generation number increases up to 3.4 m/s in air velocity because the heat capacity rate is equalized at 7.1 L/min of CFR, and then it decreases thereafter. Additionally, at 7.1 L/min of CFR and 12.8 m/s of air velocity, the HNF of spherical-platelet composition generates 6.12% more entropy than cylindrical-platelet, and 5.2 % more entropy than cylindrical-platelet, respectively. Furthermore, as the volume fraction varies, the spherical-platelet HNF exhibits a 1.4% lower entropy generation number in a wavy fin radiator compared to the cylindrical-platelet HNF, which has a 1.6% volume fraction.

## Effect of parameters on coolant exit temperature and second law efficiency

The results of the second law analysis show that the thermal system is well-designed. The efficiency according to the second law and the relationship between the coolant exit temperature, CFR, air velocity, and volume fraction of the HNF are shown in figure 15 to figure 18 for the wavy fin radiator. As CFR increases, the energy release rate decreases due to the higher coolant velocity, which causes the coolant exit temperature to drop and remain low. The coolant exit temperature rises asymptotically and nearly independently of nanoparticle form as the CFR grows because the coolant heat-releasing capacity decreases with greater CFR. The spherical-platelet-based HNF is 1.7 °C hotter than the cylindrical-platelet HNF and 1.1 °C hotter than the spherical-cylindrical HNF at a lower flow rate of 7.1 L/min. However, the coolant exit temperature drops as nanoparticles are added because more particles result in more heat transfer owing to higher thermal conductivity. Additionally, at a volume fraction of 1.6% for the HNF, the results showed that blade-platelet experienced a maximum temperature decrease of 1.7 °C, while spherical-cylindrical HNF experienced a maximum drop of 3.2 °C.

The exit temperature of the coolant is reduced, and heat transfer is increased when the air velocity increases due to the increased turbulence. At an air velocity of 12.8 m/s, the coolant exits temperature of the spherical-platelet HNF is 1.8 °C higher than that of the cylindrical-platelet hybrid and the spherical-cylindrical hybrid is 1.6 °C higher. At the same air velocity, a spherical-platelet HNF has a 6.2% higher irreversibility than a cylindrical-platelet HNF, although this difference is only noticeable as the irreversibility increases with increasing air velocity. Additionally, when the volume percentage and coolant flowrate of the HNF grow, the second law efficiency also improves. This is because the exergy gains of the air and coolant both rises as a function of these variables. At a flow rate of 7.1 L/min, the results showed that the second law efficiency of the spherical-platelet HNF was 1.12% greater than that of the cylindrical-platelet HNF. The efficiency of the cylindrical-platelet HNF composition is 0.7% higher than

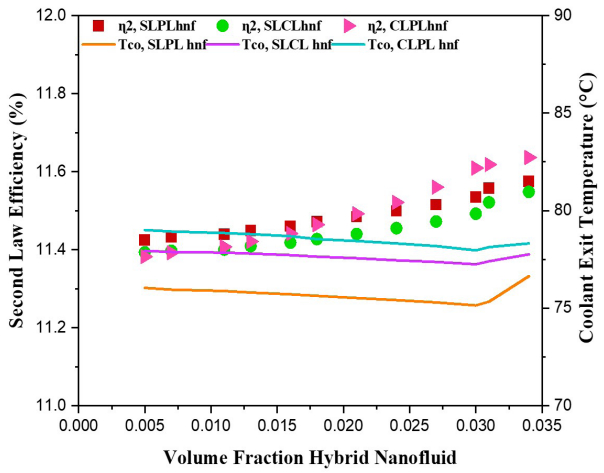



**Figure 15:** Coolant exit temperature and second law efficiency with volume fraction of HNF.

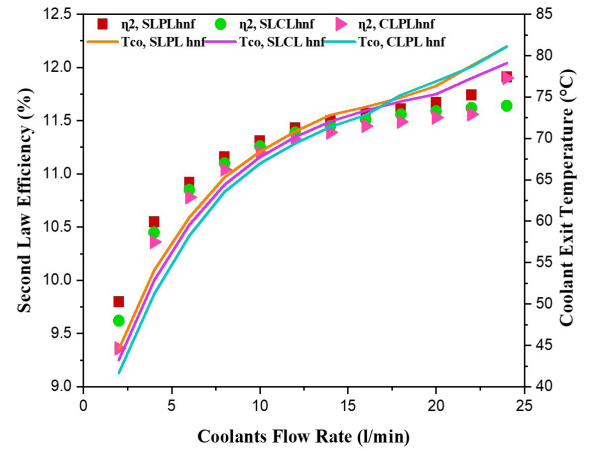



**Figure 16:** Coolant exit temperature and second law efficiency with CFR.

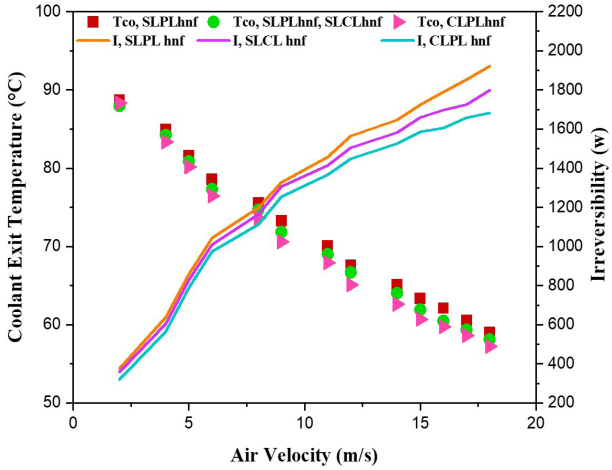



**Figure 17:** Coolant exit temperature and irreversibility with air velocity.

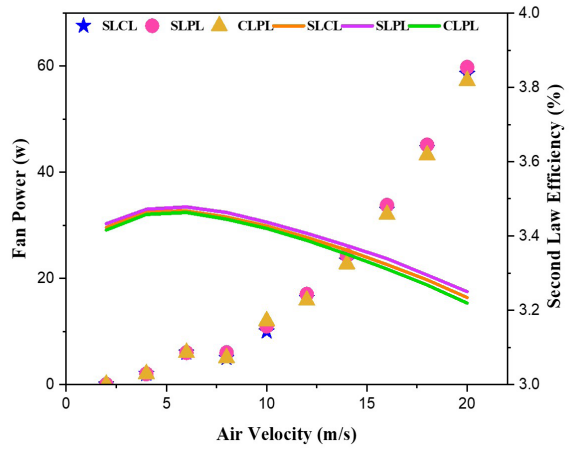



**Figure 18:** Fan power and second law efficiency with air velocity.

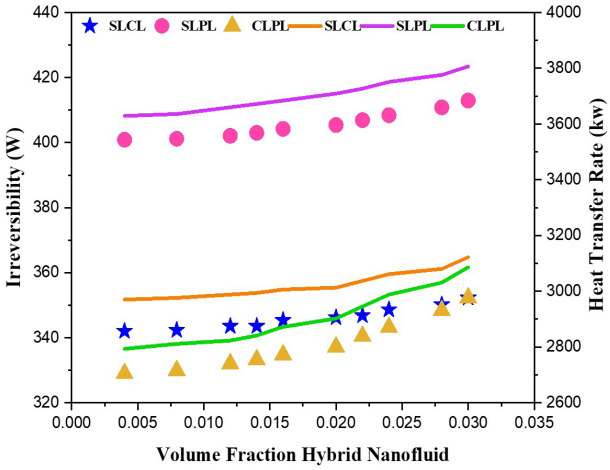



**Figure 19:** Irreversibility and heat transfer rate with volume fraction of HNF.

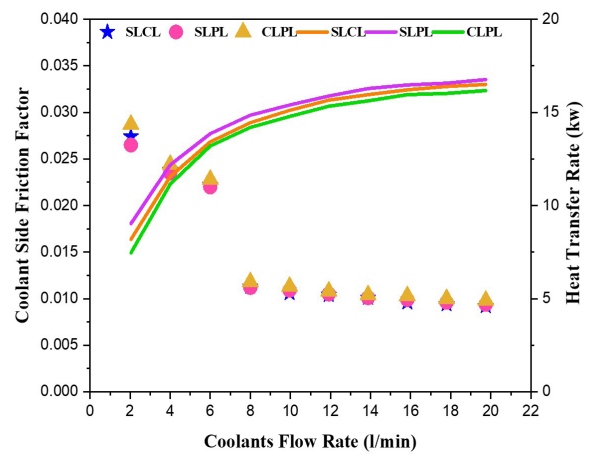



**Figure 20:** Friction factor and heat transfer rate using CFR.

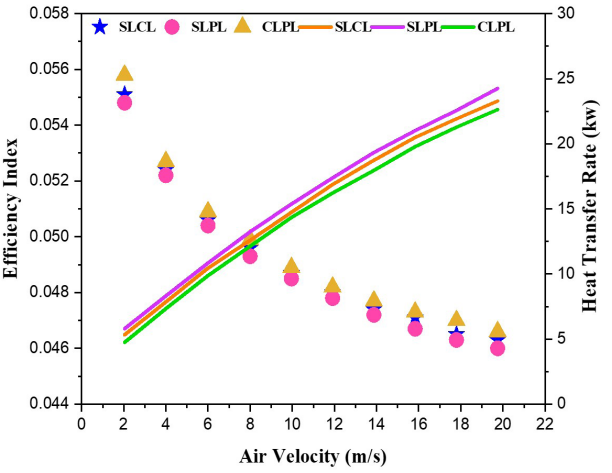



**Figure 21:** Efficiency index and heat transfer rate with air velocity.

that of the spherical-platelet hybrid composition at 1.6% volume fraction.

Figure 15 shows that the exergy efficiency decreases when air velocity increases beyond 4.9 m/s, whereas the second law efficiency initially increases with increasing air velocity. Particle shape also showed a little effect of fan power on air velocity increment, and fan power changed parabolic on-air velocity variation. Even though the cylindrical-platelet shape-based HNF achieved the minimal second law efficiency, the spherical-platelet mixture had a 1.6% improvement. This could be because air serves as a supplementary cooler and keeps the HNF in indirect touch with itself.

## Effect of parameters on heat transfer rate, irreversibility, and efficiency index

The addition of nanoparticles to an already highly irreversible water base fluid increases its irreversibility even further. As seen in figure 19, the irreversibility grows as the volume percentage of the HNF increases. The spherical-platelet HNF outperformed the spherical-cylindrical HNF in terms of irreversibility at 1.6% volume fraction, mainly because of its higher entropy. Figure 19, figure 20, and figure 21 display the change in heat transfer rate as a function of air velocity, hydraulic diameter of 0.01 m, CFR, and HNFs volume percentage for fin radiator.

As both the air velocity and the CFR rise, the turbulence effect increases, leading to a better heat efficiency index and a progressive increase in the heat transfer rate. At lower air velocities, the shape of the nanofluid has no effect on the efficiency index, but this might change at higher air speeds because of the increased CF. Furthermore, micro-level convection is enhanced by nanoparticle addition, and heat transmission is enhanced by nanoparticle impact. Thus, at a CFR of 7.1 L/min and a speed of air velocity of 12.8 m/s, the spherical-cylindrical HNF had an intermediate response, while the cylindrical-platelet hybrid had a 3.9% and 4.3% greater heat transfer, respectively.

There is a direct correlation between the friction factor and the pressure drop of the coolant, therefore a lower friction factor results in a smaller pressure drop. At a CFR of 7.1 L/min, the spherical-platelet shape of the HNF had a 3.5% lower friction factor than the cylindrical-platelet shape. Figure 21

shows the fluctuation of the CF and friction factor of the airside, which are necessary for a dimensionless efficiency index. The ratio between the CF and the airside pressure drop reduces as air velocity increases, but both factors do increase. At 2 m/s air velocity, the results showed that the cylindrical-platelet HNF had a 3.03% better efficiency index, but at greater air velocity, the form of the nanoparticle had no effect on the efficiency index.

## Conclusions

The present study examines the theoretical energy and exergy of a wavy fin radiator that uses a water-based coolant containing nanoparticles of various shapes, including cylindrical (CNT)-platelet (graphene), spherical (SiC)-platelet (graphene), and a HNF of spherical (SiC) and cylindrical (CNT). These findings are based on the analysis which was conducted under various operating situations.

- As compared to the cylindrical (CNT)-platelet (graphene) HNF at a CFR of 7.1 L/min, the spherical (SiC)-cylindrical (CNT) hybrid coolant exhibited an intermediate response, while the spherical (SiC)-platelet (graphene) nanoparticle-based hybrid coolant achieved a 5.5% higher entropy change in the air, a 3.5% higher PI, and a 3.6% higher entropy generation, respectively.
- An increase in the coolant's exergy change means that there is more exergy change in the air, which is caused by the addition of nanoparticles to the coolant. At 7.1 L/min of CFR, the exergy changes of the coolant and the exergy change in air are 3.6% and 2.9% greater, respectively, in the SiC (spherical)-graphene (platelet) composition-based HNF compared to the CNT (cylindrical)-graphene (platelet) HNF.
- Spherical (SiC)-platelet (graphene) HNF has a 1.12% higher second law efficiency at 7.1 L/min CFR, a 0.7 % higher volume fraction, and 12.8 m/s of air velocity compared to cylindrical (CNT)-platelet (graphene) HNF at the same conditions as a 1.6% volume fraction and 7.1 L/min CFR, respectively. There is a 6.2% increase in irreversibility and a 17.2% increase in volume fraction for the spherical (SiC)-platelet (graphene) HNF compared at 12.8 m/s air velocity and 1.6% volume fraction, respectively.
- Due to its 3.9% higher heat transfer rate and 4.3% higher air velocity in a wavy fin radiator at a CFR of 7.1 L/min and 12.89 m/s, respectively, and little penalty of pump and fan work, the spherical (SiC)-platelet (graphene) HNF coolant is more suitable for the practical application than the cylindrical (CNT)-platelet (graphene) HNF.

## Acknowledgements

None.

## Conflict of Interest

None.

## References

1. Liu H, Xie C, Chen G, Cao Z. 2020. Research on heat dissipation design method for motor controller radiator. *Proc Inst Mech Eng Part C J Mech Eng Sci* 234(8): 1673-1685. https://doi.org/10.1177/0954406219893723
2. Ladeinde F. 2022. An assessment of dynamic and steady state solutions of two-phase flows in a radiator heat exchanger. In AIAA Aviation Forum, Chicago, USA.
3. Ding Y, Zhang W, Deng B, Gu Y, Liao Q, et al. 2022. Experimental and numerical investigation on natural convection heat transfer characteristics of vertical 3-D externally finned tubes. *Energy* 239: 122050. https://doi.org/10.1016/j.energy.2021.122050
4. Barai R, Kumar D, Wankhade A. 2021. Heat transfer performance of nanofluids in heat exchanger: a review. *J Therm Eng* 9(1): 86-106. https://doi.org/10.18186/thermal.1243398
5. Rahmati AR, Gheibi A. 2020. Experimental and numerical analysis of a modified hot water radiator with improved performance. *Int J Therm Sci* 149: 106175. https://doi.org/10.1016/j.ijthermalsci.2019.106175
6. Yu J, Chen L, Qi C, Zhang W, Liang L. 2023. Effects of shark bionic V-groove structures and nanofluids on thermal management of electronic components. *Colloids Surf A Physicochem Eng Asp* 679: 132639. https://doi.org/10.1016/j.colsurfa.2023.132639
7. Mishra AK, Pan W, Giannelis EP, Shepherd RF, Wallin TJ. 2021. Making bioinspired 3D-printed autonomic perspiring hydrogel actuators. *Nat Protoc* 16(4): 2068-2087. https://doi.org/10.1038/s41596-020-00484-z
8. DeBortoli N, Douglass N, Warburton D, Price J, Cannon J, et al. 2022. A novel dynamic cubesat radiator design with annular geometry and varied thickness profiles. In Heat Transfer Summer Conference, Philadelphia, Pennsylvania, USA.
9. Mittal A, Misra A, Sharma A, Gupta A, Ansari N. 2020. Design and analysis of modified radiator fins to improve overall cooling efficiency. *SAE Tech Pap* 1-9. https://doi.org/10.4271/2020-01-2029
10. Bérut E, Lips S, Sartre V, Joffre T, Lefèvre F. 2023. Interconnected hollow fins to eliminate capillary blockage in vapor chamber condensers. *Appl Therm Eng* 231: 120873. https://doi.org/10.1016/j.applthermaleng.2023.120873
11. Vakrilov NV, Kafadarova NM. 2020. Thermal design: basic stages, problems and solutions. In XI National Conference with International Participation, Sofia, Bulgaria.
12. Wu P, Fang R, Dai X, Putri AAA. 2021. Analysis and optimization of heat dissipation characteristics of high-power led. In Proceedings of the 6th International Conference on Intelligent Information Processing, Bucharest, Romania.
13. Majmader FB, Hasan MJ. 2023. Thermal enhancement and entropy generation of an air-cooled 3D radiator with modified fin geometry and perforation: a numerical study. *Case Stud Therm Eng* 52: 103671. https://doi.org/10.1016/j.csite.2023.103671
14. Taler D, Taler J, Trojan M. 2020. Thermal calculations of plate–fin–and-tube heat exchangers with different heat transfer coefficients on each tube row. *Energy* 203: 117806. https://doi.org/10.1016/j.energy.2020.117806
15. Jeremiah R, Pushparaj JP, Leonard AJ, Lokeshkumar PJ, Ameen JF. 2022. Optimization of parameters to improve effectiveness of plate and fin heat exchangers using Taguchi method and CFD analysis. *Int J Veh Struct Syst* 14(3): 397. https://doi.org/10.4273/ijvss.14.3.23
16. Iwata N, Nakanoya S, Nakamura N, Takeda N, Tsutsui F. 2022. Thermal performance evaluation of space radiator for single-phase mechanically pumped fluid loop. *J Spacecraft Rockets* 59(1): 225-235. https://doi.org/10.2514/1.A35030
17. Liu Z, Cheng K, Yin Z, Wang Z, Wang J, et al. 2022. Evaluation of the CBC-ORC energy system in lunar base: working fluid combination selection, day and night operation performance. *Energy Convers Manage* 257: 115445. https://doi.org/10.1016/j.enconman.2022.115445

18. Jain J, Rajagopal T, Selvaraj A, Devaraj E. 2022. Cross-flow radiator design using CFD for FSAE car cooling system and its experimental validation using the GEMS data acquisition system. *SAE Tech Paper* 1-11. https://doi.org/10.4271/2022-01-0374
19. Ullah S, De la Sen M, Ali A, Din ZU. 2023. Investigation of the stretching/shrinking of a convective-radiative radial fin. *Int J Energy Res* 2023: 2044273. https://doi.org/10.1155/2023/2044273
20. Wang XW, Zhang ZG, Zheng LY, Wang SL, Gao K, et al. 2022. Design of waste heat discharge system and research on flow and heat transfer characteristics for space nuclear reactor. In International Conference on Nuclear Engineering, Virtual.
21. Dong Z, Li X, Li Z, Hou Y. 2020. Modeling simulation and temperature control on thermal characteristics of airborne liquid cooling system. *IEEE Access* 8: 113112-113120. https://doi.org/10.1109/ACCESS.2020.2997676
22. Khalili H, Ahmadi P, Ashjaee M, Houshfar E. 2023. Thermal analysis of a novel cycle for battery pre-warm-up and cool down for real driving cycles during different seasons. *J Therm Anal Calorim* 148(16): 8175-8193. https://doi.org/10.1007/s10973-022-11601-3
23. Sahoo RR, Kumar V. 2021. Impact of novel dissimilar shape ternary composition-based hybrid nanofluids on the thermal performance analysis of radiator. *J Therm Sci Eng Appl* 13(4): 041002. https://doi.org/10.1115/1.4048668
24. Sahoo RR. 2021. Effect of various shape and nanoparticle concentration based ternary hybrid nanofluid coolant on the thermal performance for automotive radiator. *Heat Mass Transfer* 57(5): 873-887. https://doi.org/10.1007/s00231-020-02971-1